



**HAL**  
open science

## Sub-oxycline methane oxidation can fully uptake CH<sub>4</sub> produced in sediments: case study of a lake in Siberia

Frédéric Thalasso, Armando Sepulveda-Jauregui, Laure Gandois, Karla Martinez-Cruz, Oscar Gerardo-Nieto, María Astorga-España, Roman Teisserenc, Céline Lavergne, Nikita Tananaev, Maialen Barret, et al.

### ► To cite this version:

Frédéric Thalasso, Armando Sepulveda-Jauregui, Laure Gandois, Karla Martinez-Cruz, Oscar Gerardo-Nieto, et al.. Sub-oxycline methane oxidation can fully uptake CH<sub>4</sub> produced in sediments: case study of a lake in Siberia. *Scientific Reports*, 2020, 10 (1), 10.1038/s41598-020-60394-8. hal-03147113

**HAL Id: hal-03147113**

**<https://amu.hal.science/hal-03147113>**

Submitted on 19 Feb 2021

**HAL** is a multi-disciplinary open access archive for the deposit and dissemination of scientific research documents, whether they are published or not. The documents may come from teaching and research institutions in France or abroad, or from public or private research centers.

L'archive ouverte pluridisciplinaire **HAL**, est destinée au dépôt et à la diffusion de documents scientifiques de niveau recherche, publiés ou non, émanant des établissements d'enseignement et de recherche français ou étrangers, des laboratoires publics ou privés.



Distributed under a Creative Commons Attribution 4.0 International License

OPEN

# Sub-oxycline methane oxidation can fully uptake CH<sub>4</sub> produced in sediments: case study of a lake in Siberia

Frédéric Thalasso<sup>1,2</sup>, Armando Sepulveda-Jauregui<sup>2,3\*</sup>, Laure Gandois<sup>4</sup>, Karla Martinez-Cruz<sup>2</sup>, Oscar Gerardo-Nieto<sup>1</sup>, María S. Astorga-España<sup>2</sup>, Roman Teisserenc<sup>4</sup>, Céline Lavergne<sup>5</sup>, Nikita Tananaev<sup>6</sup>, Maialen Barret<sup>4</sup> & Léa Cabrol<sup>7</sup>

It is commonly assumed that methane (CH<sub>4</sub>) released by lakes into the atmosphere is mainly produced in anoxic sediment and transported by diffusion or ebullition through the water column to the surface of the lake. In contrast to that prevailing idea, it has been gradually established that the epilimnetic CH<sub>4</sub> does not originate exclusively from sediments but is also locally produced or laterally transported from the littoral zone. Therefore, CH<sub>4</sub> cycling in the epilimnion and the hypolimnion might not be as closely linked as previously thought. We utilized a high-resolution method used to determine dissolved CH<sub>4</sub> concentration to analyze a Siberian lake in which epilimnetic and hypolimnetic CH<sub>4</sub> cycles were fully segregated by a section of the water column where CH<sub>4</sub> was not detected. This layer, with no detected CH<sub>4</sub>, was well below the oxycline and the photic zone and thus assumed to be anaerobic. However, on the basis of a diffusion-reaction model, molecular biology, and stable isotope analyses, we determined that this layer takes up all the CH<sub>4</sub> produced in the sediments and the deepest section of the hypolimnion. We concluded that there was no CH<sub>4</sub> exchange between the hypolimnion (dominated by methanotrophy and methanogenesis) and the epilimnion (dominated by methane lateral transport and/or oxic production), resulting in a vertically segregated lake internal CH<sub>4</sub> cycle.

Methane (CH<sub>4</sub>) released from lakes to the atmosphere is generally assumed to be produced in anoxic sediment and transported by diffusion or ebullition through the water column<sup>1,2</sup>, where it is subject to oxidation, generally identified as a major sink<sup>2-5</sup>. In stratified lakes, the diffusion barrier formed by the thermocline promotes CH<sub>4</sub> storage in the hypolimnion. The stored CH<sub>4</sub> is released mainly to the epilimnion and then to the atmosphere during water column overturn<sup>6,7</sup>. Lateral transport of CH<sub>4</sub> from the littoral to the pelagic zones may also substantially modify the CH<sub>4</sub> balance at the epilimnion of the lakes<sup>1,8,9</sup>. Although this has been the prevailing theory, several other CH<sub>4</sub> cycle processes have been discovered. For instance, CH<sub>4</sub> production in the epilimnion under aerobic conditions has been observed in several aquatic ecosystems<sup>8,10-13</sup>. Another process previously reported is CH<sub>4</sub> oxidation below the oxycline, which is typically associated with microaerophilic conditions<sup>4</sup>, oxygenic photosynthesis<sup>4,14</sup>, or, in some cases, assumed to be anaerobic<sup>15</sup>. These processes explain why deviations to standard CH<sub>4</sub> concentration profiles (usually decreasing from the bottom to the surface) are often observed as concentrations increase or decrease in local areas.

In this study, we observed an atypical CH<sub>4</sub> profile in a strongly stratified lake (Sila Lake) in north-central Siberia. From the bottom to the surface, the profile showed a sharp decrease of the CH<sub>4</sub> concentration below the detection limit of our method (5 nmol L<sup>-1</sup>) in the benthic zone of the water column, well below the oxycline and

<sup>1</sup>Biotechnology and Bioengineering Department, Center for Research and Advanced Studies (Cinvestav), Mexico City, Mexico. <sup>2</sup>The Environmental Biogeochemistry in Extreme Ecosystems Laboratory (EnBEElab), University of Magallanes, Punta Arenas, Chile. <sup>3</sup>Center for Climate and Resilience Research (CR)2, Santiago, Chile. <sup>4</sup>EcoLab, Université de Toulouse, CNRS, Toulouse, France. <sup>5</sup>Escuela de Ingeniería Bioquímica, Pontificia Universidad de Valparaíso, Valparaíso, Chile. <sup>6</sup>Melnikov Permafrost Institute, Yakutsk, Russia. <sup>7</sup>Aix-Marseille University, Univ Toulon, CNRS, IRD, Mediterranean Institute of Oceanography, Marseille, France. \*email: [armando.sepulveda@umag.cl](mailto:armando.sepulveda@umag.cl)

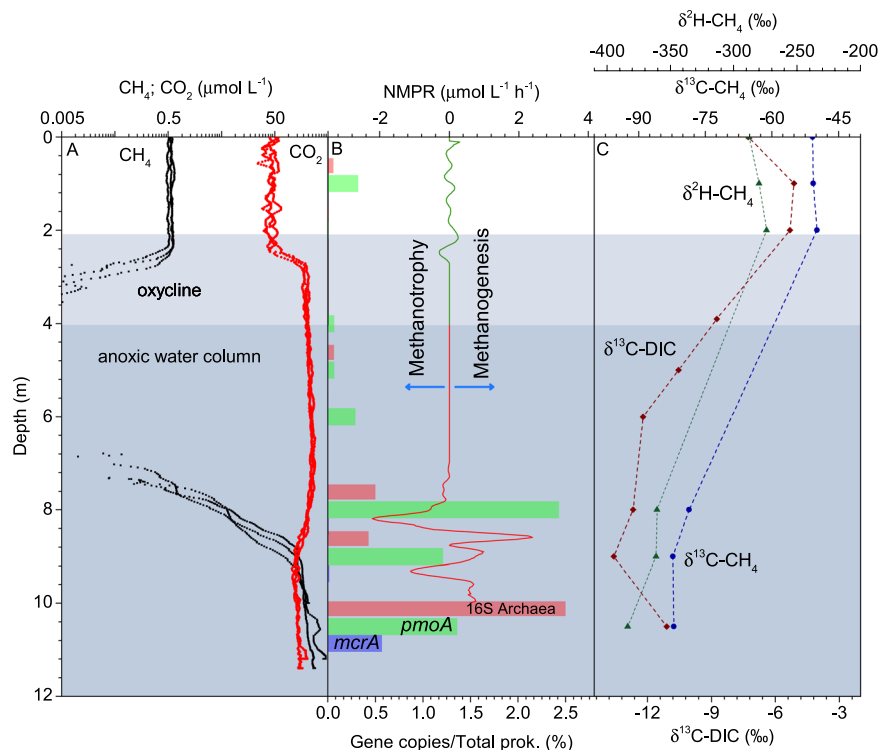


**Figure 1.** (A) Depth profiles of dissolved  $\text{CH}_4$  ( $C_{\text{CH}_4}$ ) and  $\text{CO}_2$  ( $C_{\text{CO}_2}$ ) in logarithmic scale; (B) net methane production rates of one profile (for clarity purposes, replicate profiles are shown in Fig. S3); and relative abundance, in reference to total prokaryotes, of *pmoA* genes (green bars), *mcrA* genes (blue bars) and total archaea genes (pink bars). Epilimnion NMPR are multiplied by 1000; (C)  $\delta^{13}\text{C-DIC}$  (brown square),  $\delta^{13}\text{C-CH}_4$  (green circles), and  $\delta^2\text{H-CH}_4$  (blue triangles).

the photic zone, and showed an increase in  $\text{CH}_4$  concentration in the aerobic epilimnion. This profile was created using a high resolution, high sensitivity method<sup>16,17</sup> which allowed the net methane production and oxidation rates to be determined using a diffusion-reaction model, showing a short distance transition between both processes in the hypolimnion. This  $\text{CH}_4$  concentration profile was correlated to methanotroph and methanogenic archaea abundances determined by *pmoA* and *mcrA* gene qPCR, respectively.

## Results and Discussion

The depth measurements collected were used to develop a bathymetric map (Fig. S1) that shows a maximum depth of 12 m in the southeastern branch of the lake. Satellite imagery (Google Earth Engine) was used to determine that the area of the lake was 3.6 Ha. Combining the area of the lake and the bathymetric map, we constructed a hypsometric histogram to estimate the total water volume of the lake to be 168,000  $\text{m}^3$ . The lake was strongly stratified, with a mean surface temperature of  $16.5 \pm 0.7^\circ\text{C}$  (mean  $\pm$  one standard deviation), a bottom temperature of  $3.4 \pm 0.3^\circ\text{C}$ , a thermocline 2–4 m deep, and a maximum gradient of  $8.6^\circ\text{C m}^{-1}$  (Fig. S2). The oxycline matched the thermocline and anoxic conditions (i.e., dissolved oxygen (DO) concentration below  $0.3 \mu\text{mol L}^{-1}$ ) were found at depths below 4 m. The Secchi depth was  $1.8 \pm 0.15$  m, meaning that the euphotic depth ( $Z_{1\%}$ ), i.e., depth at which the photosynthetically available radiation was 1% of its surface value, was estimated at  $4.9 \pm 0.4$  to  $5.6 \pm 0.4$  m.

In addition to each sampling and monitoring station, the profiles of dissolved  $\text{CH}_4$  and carbon dioxide ( $\text{CO}_2$ ) concentration ( $C_{\text{CH}_4}$  and  $C_{\text{CO}_2}$ , respectively) were measured in triplicate at the center of the lake (P1, see materials and methods, Fig. 1A). Epilimnetic  $C_{\text{CH}_4}$  and  $C_{\text{CO}_2}$ , at depths between 0 and 2.5 m, were  $0.56 \pm 0.05 \mu\text{mol L}^{-1}$  and  $44 \pm 7 \mu\text{mol L}^{-1}$ , respectively. Below 2.5 m,  $C_{\text{CH}_4}$  rapidly decreased and was no longer detected below depths of  $2.96 \pm 0.13$  m (until depths greater than 7 m). On the contrary, an increase of  $C_{\text{CO}_2}$  was observed to  $209 \pm 16 \mu\text{mol L}^{-1}$ . At a depth of  $7.12 \pm 0.14$  m, well below the oxycline and  $Z_{1\%}$ ,  $C_{\text{CH}_4}$  rapidly increased and reached  $196 \pm 18 \mu\text{mol L}^{-1}$  at 10 m. Higher values were observed below 10 m but these measurements were discarded as potentially being the result of sediment disturbances, at a depth of 10.4–10.7 m. Inversely,  $C_{\text{CO}_2}$  decreased in the deepest section of the hypolimnion to  $135 \pm 11 \mu\text{mol L}^{-1}$  at 10 m. The section of the water column where  $\text{CH}_4$  was not detected (3–7 m), called the “methane minimum zone” (MMZ), expanded along the transversal and longitudinal transects (Fig. 2), and acted as a segregation zone between the hypolimnetic and the epilimnetic  $\text{CH}_4$ .

To better characterize the  $\text{CH}_4$  profiles observed, a diffusion-reaction model was applied to estimate net methane production rates (NMPR; Fig. 1B, S3D–F) and vertical fluxes through the water column (Fig. S3A–C). As shown in the diagram, a peak of negative NMPR, i.e.,  $\text{CH}_4$  sink, was observed below the MMZ, immediately above a peak of positive NMPR, i.e.,  $\text{CH}_4$  source. The same pattern was observed in the three replicates (Fig. S3),

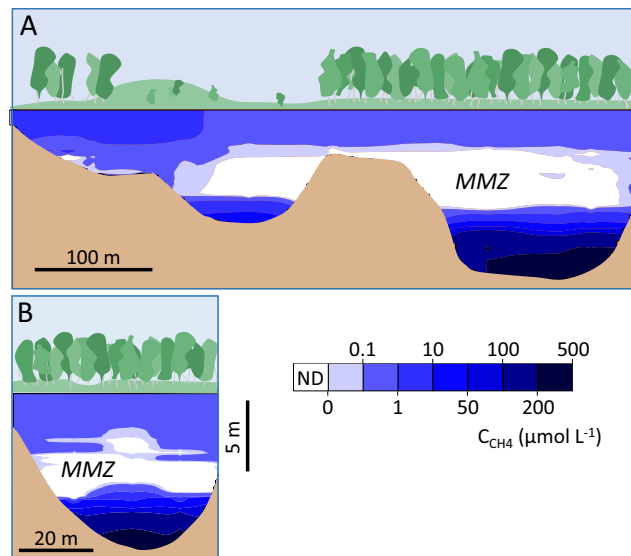


**Figure 2.** Longitudinal (east-west; **A**) and transversal (north-south; **B**) transectional maps of dissolved  $\text{CH}_4$  concentration showing the expansion of the minimum methane zone (MMZ). ND stands for not detected.

although with differences in depths (maximum difference of 0.54 m between the three negative NMPR peaks), which were likely caused by boat motion and inaccurate positioning, evidenced by differences in water column depth varying between 10.4 and 10.7 m. It is noteworthy that the depth intervals between  $\text{CH}_4$  sink and source peaks were consistently small,  $0.51 \pm 0.11$  m, indicating a sudden shift in the dominant  $\text{CH}_4$  process. The average minimum and maximum NMPR corresponding to the first methanotrophic and the methanogenic peaks, in a downward direction, were  $-1.82 \pm 0.34$  and  $1.69 \pm 0.68 \mu\text{mol L}^{-1} \text{h}^{-1}$ , respectively, which suggests that the magnitude of both processes was comparable.

The isotopic signature of  $\text{CH}_4$  and the  $\text{CH}_4$  production fractionation factor ( $\alpha$ ; see materials and methods), show two homogeneous zones (Fig. 1C). In the hypolimnetic layer, depleted  $\delta^{13}\text{C}-\text{CH}_4$  ( $-78.6$  to  $-82.2\text{‰}$ ) and  $\delta^2\text{H}-\text{CH}_4$  ( $-360$  to  $-383\text{‰}$ ), coupled to relatively high  $\alpha$  values (1.072 to 1.077), strongly support hydrogenotrophic production of  $\text{CH}_4$  from  $\text{CO}_2$ <sup>12,18</sup>. On the contrary, at the epilimnion, enriched values of  $\delta^{13}\text{C}-\text{CH}_4$  ( $-49.8$  to  $-50.8\text{‰}$ ) and  $\delta^2\text{H}-\text{CH}_4$  ( $-274.2$  to  $-287.8\text{‰}$ ), coupled with relatively low  $\alpha$  values (1.046 to 1.048), are consistent with a predominance of acetoclastic production of  $\text{CH}_4$ <sup>12,18</sup>. Indeed, according to Whiticar and Faber<sup>19</sup>,  $\alpha$  from 1.055 to 1.09 most likely corresponds to hydrogenotrophic methanogenesis, while  $\alpha$  from 1.04 to 1.055 corresponds to acetoclastic methanogenesis.

The abundance of methane oxidizing bacteria (MOB) quantified through the relative abundance of *pmoA* gene (Fig. 1B) was minimal in the MMZ, representing  $<0.03\%$  of the prokaryotic community, as expected from the absence of detectable levels of  $\text{CH}_4$ . Higher abundance of MOB was detected within the anoxic water column (8–10 m), where MOB represented from 1.1% to 2.5% of the total community. Notably, the peak of MOB abundance was found at 8 m depth ( $1.6 \pm 0.05 \times 10^8$  *pmoA* copies  $\text{L}^{-1}$ ), which coincided with the depth of maximum methanotrophic activity (Fig. 1B, S3), suggesting that MOB were potentially major contributors to the  $\text{CH}_4$  oxidation in this lake. This is not surprising since the possible involvement of aerobic methanotrophs in anaerobic methane oxidation has been previously suggested<sup>4,20,21</sup>. Although MOB activity was not determined, this finding indicates that MOB might be active in anoxic waters. Quantitative PCR also revealed that the amount of *mcrA* gene was minimal in the MMZ and remained low where the methanotrophic peak was observed, being two orders of magnitude less abundant than the *pmoA* gene (Fig. 1B). This result suggests that *mcrA*-carrying anaerobic methane oxidizing archaea (ANME) were not major contributors to the strong methane oxidation observed in this anoxic layer. The *mcrA* gene abundance only increased significantly at the bottom of the water column ( $1.1 \times 10^7 \pm 0.3 \times 10^7$  *pmoA* copies  $\text{L}^{-1}$  at 10 m depth); similar results were observed with total archaea (quantified through their 16S rRNA gene). In addition, a local *mcrA* maximum ( $2.3 \times 10^5 \pm 0.4 \times 10^5$  copies  $\text{L}^{-1}$ ) was observed in the oxic epilimnion at a depth of 2 m, which indicates the presence of methanogens despite the oxic environment.

The major  $\text{CH}_4$  oxidation observed in the anoxic epilimnion raises the important question of the oxic or anoxic nature of the process. Several arguments suggest the absence of oxygen, either diffused from the top or locally produced. First, the euphotic depth of 4.9–5.6 m was 2.9–3.6 m above the peak of methanotrophic activity, where the photosynthetic available radiation was 0.03–0.08% of its surface value. Second, the peak of methanotrophic activity of  $1.82 \pm 0.34 \mu\text{mol CH}_4 \text{L}^{-1} \text{h}^{-1}$  would require  $3.64 \pm 0.68 \mu\text{mol O}_2 \text{L}^{-1} \text{h}^{-1}$ , i.e., two moles of  $\text{O}_2$  required to oxidize one mole of  $\text{CH}_4$ . That oxygen requirement is within the higher range of primary production reported for the euphotic or epilimnion zones of 118 lakes<sup>22</sup> worldwide, thus unlikely to occur 2.9–3.6 m below the euphotic depth. Third, the average methanotrophic activity over the entire water column, determined by integration of negative NMPR, corresponded to  $611 \pm 80 \mu\text{mol CH}_4 \text{m}^{-2} \text{h}^{-1}$ . That figure would require a counter flux of  $1,222 \pm 160 \mu\text{mol O}_2 \text{m}^{-2} \text{h}^{-1}$ . According to a maximum hypolimnetic diffusivity of  $2.819 \text{m}^2 \text{h}^{-1}$ <sup>123</sup>, the DO

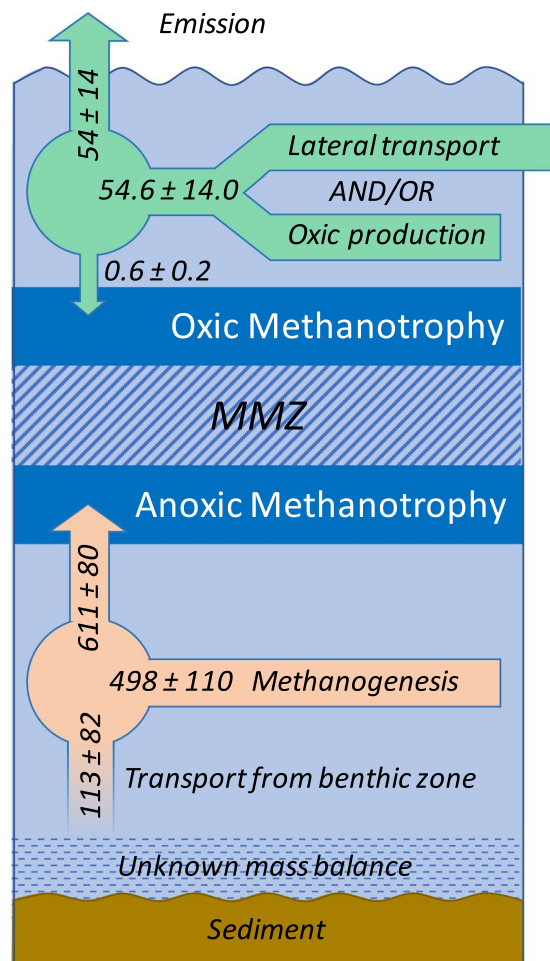


**Figure 3.**  $\text{CH}_4$  mass balance in the water column of Sila Lake. Arrows indicate  $\text{CH}_4$  transport and production while numbers indicate the magnitude of these processes, all of which are expressed per unit of lake area ( $\mu\text{mol CH}_4 \text{ m}^{-2} \text{ h}^{-1}$ ). The minimum methane zone is called MMZ.

gradient along the water column, required to sustain aerobic methanotrophy, corresponds to  $433 \mu\text{mol L}^{-1}$  per meter of water column depth, which is incompatible with the measured DO concentration in the hypolimnion; i.e., below  $0.3 \mu\text{mol L}^{-1}$ . Fourth, the proximity of methanogenic peaks, observed  $0.51 \pm 0.11 \text{ m}$  below the methanotrophic peak, does not support a sudden shift from an active oxic to a strict anaerobic process. The unlikelihood of aerobic  $\text{CH}_4$  oxidation raises the question of the electron acceptor as an alternative to  $\text{O}_2$ . No evidence arises from nitrate or nitrite (Table S2), as none of these electron acceptors for anaerobic methane oxidation<sup>20,24</sup> showed a significant concentration change in the region where methanotrophic activity was found, and both nitrate or nitrite in the lake water column were below or at the lower range of concentration to support AOM coupled to denitrification<sup>25</sup>. Thus, the present work does not reveal the possible electron acceptors for AOM in the epilimnion of the lake, since sulfate, oxidized metals, and organic matter<sup>26</sup> were not tested.

Our results show that the MMZ segregates two different  $\text{CH}_4$  zones of the water column with no diffusive exchange between them. The existence of an MMZ segregation zone is supported not only by the  $\text{CH}_4$  profiles, discarding diffusive transfer between the epilimnion and the hypolimnion, but also by the  $\text{CH}_4$  isotopic signature, suggesting different  $\text{CH}_4$  origins in each zone. However, despite segregation between the epilimnion and the hypolimnion, bubbles formed in the sediments might transfer  $\text{CH}_4$  to the epilimnion during their migration to the surface of the lake. Nevertheless, at each sampling and monitoring station,  $\text{CH}_4$  and  $\text{CO}_2$  fluxes were determined in triplicate with a dynamic closed chamber coupled to a greenhouse gas analyzer (UGGA 30 P, Los Gatos Research, CA, USA; data acquisition frequency of  $1 \text{ s}^{-1}$  and  $\text{CH}_4$  sensitivity of 30 ppb)<sup>17</sup>. During a total of 54 flux measurements over a total time of 4.5 h, no evidence of bubbling was found; i.e., peak increase of  $\text{CH}_4$  concentration within the chamber<sup>17</sup>. Bubbles were only occasionally visually observed in the littoral region at the western section of the lake. Thus, ebullitive transfer of  $\text{CH}_4$  from the hypolimnion to the epilimnion, is unlikely although not discountable. The  $\text{CH}_4$  found at the epilimnion might be considered as the product of local oxic production and/or lateral transport from the littoral zone<sup>1,8,10–13</sup>.

We estimated the flux, downward to the MMZ, as  $0.62 \pm 0.15 \mu\text{mol CH}_4 \text{ m}^{-2} \text{ h}^{-1}$  (Fig. S3 A–C). A triplicate measurement of the  $\text{CH}_4$  flux to the atmosphere, at each of the three locations where the  $C_{\text{CH}_4}$  profiles were made, gave an average of  $54 \pm 14 \mu\text{mol CH}_4 \text{ m}^{-2} \text{ h}^{-1}$ . Thus, the transfer of  $\text{CH}_4$  to the MMZ was negligible and, assuming steady-state concentrations (i.e., those that did not change over time), we estimated the oxic production and/or

lateral transport to equalize flux to the atmosphere, i.e.,  $54 \pm 14 \mu\text{mol CH}_4 \text{ m}^{-2} \text{ h}^{-1}$ . Figure 3 shows the  $\text{CH}_4$  mass balance of Sila Lake at the time of characterization and indicates that about 92% of the total  $\text{CH}_4$  produced in or transported to the lake is oxidized. The steady-state assumption used to establish the  $\text{CH}_4$  mass balance might be a simplistic consideration regarding the epilimnion. Sila Lake is a northern lake with an ice-free period ranging from three to four months (personal communication with local inhabitants); this short period of summer stratification suggests relatively rapid changes of the water column structure, which is potentially contradictory to steady-state conditions. However, the total amount of  $\text{CH}_4$  present in the epilimnion, considering a depth layer of 2.3 m, was estimated to be  $1.34 \pm 0.12 \text{ mmol CH}_4 \text{ m}^{-2}$ . Dividing the amount of  $\text{CH}_4$  present in the epilimnion by the flux to the atmosphere mentioned above, we estimated the  $\text{CH}_4$  turnover time to range from 22–27 h. The latter indicates that the  $\text{CH}_4$  cycle in the epilimnion is dynamic and that the  $\text{CH}_4$  emitted to the atmosphere is rapidly replaced by lateral transport and/or oxic production.

This study shows that, in at least some cases,  $\text{CH}_4$  cycling in stratified lakes should be considered as two segregated systems with no exchange between them. While the hypolimnion is dominated by methanotrophy and hydrogenotrophic methanogenesis, the epilimnion is dominated by  $\text{CH}_4$  originating from acetoclastic production, *in situ* or transferred from surrounding terrestrial ecosystems. The segregation between the  $\text{CH}_4$  cycle in the epilimnion and the hypolimnion has been suggested by several reports<sup>5,8,10,12,13</sup> and used as a supporting evidence that epilimnetic  $\text{CH}_4$  is locally produced<sup>8,10–13,27</sup> or transported from the littoral zone<sup>1,8,28</sup>. In addition to similar conclusions, the present work was based on an innovative high resolution and sensitive method for determining  $\text{C}_{\text{CH}_4}$ , which allowed the NMPR profile to be created and demonstrated that methanotrophy can occur well below the oxycline and euphotic zone of a lake. This method also revealed the drastic shift, relative to depth, between the two opposing dominant  $\text{CH}_4$  processes of anaerobic methanogenesis and methanotrophy, with the latter being potentially anoxic or at least not associated with locally produced oxygen. Notably, *pmoA*-carrying bacteria were the major microbial contributors of methane oxidation in this lake and largely predominated (over potential ANMEs) at the depth of highest methane oxidation activity, leading to a complete exhaustion of produced methane at the hypolimnetic water column. The extent to which the behavior observed in Sila Lake can be extrapolated to other lakes is unknown but is certainly an important milestone and should be investigated further, along with the identity of the methane oxidizing bacteria potentially involved in AOM in this lake and others.

## Materials and Methods

A small, Y-shaped unnamed lake, located in a discontinuous permafrost area of northern Siberia<sup>29</sup> 5 km north of the town of Igarka, Krasnoyarsk Krai, Russia (Fig. S1), was selected and called Sila for the purpose of this study (Lat. 67.5138, Long. 86.5915). Sila Lake is of glacial origin and heavily influenced by the thermokarst. It is surrounded by northern forest and peatlands, which is the dominant landscape of the region. About one-third of the perimeter (600 m), mostly on the west, is bordered by shallow peatland, while mixed forest, i.e., larch (*Larix sibirica*), birch (*Betula pendula*), and Siberian pine (*Pinus sibirica*) borders about two-thirds of the perimeter (1100 m). In August 2016, sampling and monitoring stations were established at 13 locations along a west-east longitudinal transect and 5 locations along a transversal north-south transect (Fig. S1).  $\text{C}_{\text{CH}_4}$  and  $\text{C}_{\text{CO}_2}$  concentrations along the water column were determined using a membrane-integrated cavity output spectrometry method (M-ICOS)<sup>16</sup>. This method, described in more detail in the supporting information, allowed for the continuous measurement of dissolved gas at a frequency of  $1 \text{ s}^{-1}$ , which corresponded to approximately 50 dissolved gas concentration data points per meter of the water column. The lower detection limit of the method under the present configuration was  $5 \text{ nmol L}^{-1}$  for  $\text{C}_{\text{CH}_4}$  and  $4 \mu\text{mol L}^{-1}$  for  $\text{C}_{\text{CO}_2}$ . Vertical  $\text{CH}_4$  fluxes and NMPR within the water column were derived from the estimation of turbulent diffusion of  $\text{CH}_4$  across the concentration gradient according to the method established in Kankaala *et al.*,<sup>30</sup> details of the method are provided in the supporting information. At each location, water column parameters including pH, temperature, DO, redox potential, and conductivity were also determined at 1 m depth intervals using multi-parametric probes (HI 9828, Hanna Instrument, Mexico). Water transparency was measured with a 30 cm Secchi disk. The euphotic depth ( $Z_{1\%}$ ) was estimated according to methods established by French *et al.*<sup>31</sup> and LaPierre and Edmundson<sup>32</sup>.

At the deepest location, water samples were taken at 1, 2, 4, 5, 6, 8, 9, and 10 m with a Van Dorn Bottle. These samples were used for molecular biology, stable isotope analysis of dissolved inorganic carbon ( $\delta^{13}\text{C-DIC}$ ) and  $\text{CH}_4$  ( $\delta^2\text{H-CH}_4$  and  $\delta^{13}\text{C-CH}_4$ ). All stable isotope samples were analyzed in replicates of three and standard deviation was typically 0.2‰. The  $\delta^{13}\text{C-DIC}$  was analyzed by an Isoprime 100 unit (MultiFlow-Geo, Elementar, UK). Stable isotopic analysis of  $\text{CH}_4$  ( $\delta^2\text{H}$  and  $\delta^{13}\text{C}$ ) was completed at UC Davis' Stable Isotope Facility with a Thermo Scientific PreCon unit interfaced to a Thermo Scientific Delta V Plus Isotope Ratio Mass Spectrometer (Bremen, Germany). The fractionation factor  $\alpha$  indicates the magnitude of isotopic separation between the  $\delta^{13}\text{C}$  values of  $\Sigma\text{CO}_2$  (total dissolved inorganic carbon) and  $\text{CH}_4$  in anaerobic environments. Its value reflects the dominant  $\text{CH}_4$  production pathways. It also shows systematic shifts in  $\text{CH}_4$  oxidation processes<sup>33</sup>. It was calculated as:  $\alpha = (\delta^{13}\text{C-DIC} + 1000) / (\delta^{13}\text{C-CH}_4 + 1000)$ <sup>18</sup>. For molecular biology characterization, water samples were filtered as soon as possible after sampling (i.e. <24 h). DNA extraction was completed and quantitative PCR (qPCR) was performed to assess the abundance of the following genes: bacterial 16S rRNA gene (total bacteria), archaeal 16S rRNA gene (total archaea), *pmoA* gene (particulate methane monooxygenase) and *mcrA* gene (methyl coenzyme M reductase, indicative of methanogens and ANMEs). More details of these methods are provided in the supporting information.

## Data availability

The data analyzed in this study are available from the corresponding author upon request.

Received: 4 June 2019; Accepted: 10 February 2020;

Published online: 25 February 2020

## References

- Peeters, F., Encinas Fernandez, J. & Hofmann, H. Sediment fluxes rather than oxic methanogenesis explain diffusive CH<sub>4</sub> emissions from lakes and reservoirs. *Sci. Rep.* **9**(1), 243, <https://doi.org/10.1038/s41598-018-36530-w> (2019).
- Bastviken, D., Cole, J. J., Pace, M. L. & Van de Bogert, M. C. Fates of methane from different lake habitats: Connecting whole-lake budgets and CH<sub>4</sub> emissions. *J. Geophys. Res.* **113**, G02024, <https://doi.org/10.1029/2007JG000608> (2008).
- Martinez-Cruz, K., Sepulveda-Jauregui, A., Walter Anthony, K. & Thalasso, F. Geographic and seasonal variation of dissolved methane and aerobic methane oxidation in Alaskan lakes. *Biogeosciences* **12**(15), 4595–4606, <https://doi.org/10.5194/bg-12-4595-2015> (2015).
- Milucka, J. *et al.* Methane oxidation coupled to oxygenic photosynthesis in anoxic waters. *ISME J.* **9**(9), 1991–2002, <https://doi.org/10.1038/ismej.2015.12> (2015).
- Morana, C. *et al.* Methanotrophy within the water column of a large meromictic tropical lake (Lake Kivu, East Africa). *Biogeosciences* **12**(7), 2077–2088, <https://doi.org/10.5194/bg-12-2077-2015> (2015).
- Michmerhuizen, C. M., Striegl, R. G. & McDonald, M. E. Potential methane emission from north-temperate lakes following ice melt. *Limnol. Oceanogr.* **41**(5), 985–991, <https://doi.org/10.4319/lo.1996.41.5.0985> (1996).
- Bastviken, D., Cole, J., Pace, M. & Tranvik, L. Methane emissions from lakes: Dependence of lake characteristics, two regional assessments, and a global estimate. *Global Biogeochem. Cycles* **18**(4), GB4009, <https://doi.org/10.1029/2004GB002238> (2004).
- DelSontro, T., del Giorgio, P. A. & Prairie, Y. T. No Longer a Paradox: The Interaction Between Physical Transport and Biological Processes Explains the Spatial Distribution of Surface Water Methane Within and Across Lakes. *Ecosystems* **21**(6), 1073–1087, <https://doi.org/10.1007/s10021-017-0205-1> (2018).
- Paytan, A. *et al.* Methane transport from the active layer to lakes in the Arctic using Toolik Lake, Alaska, as a case study. *Proc. Natl. Acad. Sci.* **112**(12), 3636–3640, <https://doi.org/10.1073/pnas.1417392112> (2015).
- Tang, K. W., McGinnis, D. F., Ionescu, D. & Grossart, H.-P. Methane Production in Oxidic Lake Waters Potentially Increases Aquatic Methane Flux to Air. *Environ. Sci. Technol. Lett.* **3**(6), 227–233, <https://doi.org/10.1021/acs.estlett.6b00150> (2016).
- Donis, D. *et al.* Full-scale evaluation of methane production under oxic conditions in a mesotrophic lake. *Nat. Commun.* **8**(1), 1661, <https://doi.org/10.1038/s41467-017-01648-4> (2017).
- Bogard, M. J. *et al.* Oxic water column methanogenesis as a major component of aquatic CH<sub>4</sub> fluxes. *Nat. Commun.* **5**(1), 5350, <https://doi.org/10.1038/ncomms6350> (2014).
- Günthel, M. *et al.* Contribution of oxic methane production to surface methane emission in lakes and its global importance. *Nat. Commun.* **10**(1), 5497, <https://doi.org/10.1038/s41467-019-13320-0> (2019).
- Carini, S., Bano, N., LeClerc, G. & Joye, S. B. Aerobic methane oxidation and methanotroph community composition during seasonal stratification in Mono Lake, California (USA). *Environ. Microbiol.* **7**(8), 1127–1138, <https://doi.org/10.1111/j.1462-2920.2005.00786.x> (2005).
- Blees, J. *et al.* Micro-aerobic bacterial methane oxidation in the chemocline and anoxic water column of deep south-Alpine Lake Lugano (Switzerland). *Limnol. Oceanogr.* **59**(2), 311–324, <https://doi.org/10.4319/lo.2014.59.2.0311> (2014).
- Gonzalez-Valencia, R. *et al.* In Situ Measurement of Dissolved Methane and Carbon Dioxide in Freshwater Ecosystems by Off-Axis Integrated Cavity Output Spectroscopy. *Environ. Sci. Technol.* **48**(19), 11421–11428, <https://doi.org/10.1021/es500987j> (2014).
- Sepulveda-Jauregui, A., Martinez-Cruz, K., Lau, M. & Casper, P. Assessment of methane and carbon dioxide emissions in two sub-basins of a small acidic bog lake artificially divided 30 years ago. *Freshwater Biol.* **63**, 1534–1549, <https://doi.org/10.1111/fwb.13182> (2018).
- Blaser, M. & Conrad, R. Stable carbon isotope fractionation as tracer of carbon cycling in anoxic soil ecosystems. *Curr. Opin. Biotechnol.* **41**(8), 122–129, <https://doi.org/10.1016/j.copbio.2016.07.001> (2016).
- Whiticar, M. J. & Faber, E. Methane oxidation in sediment and water column environments - isotope evidence. *Org. Geochem.* **10**, 759–768, [https://doi.org/10.1016/s0146-6380\(86\)80013-4](https://doi.org/10.1016/s0146-6380(86)80013-4) (1986).
- Martinez-Cruz, K. *et al.* Anaerobic oxidation of methane by aerobic methanotrophs in sub-Arctic lake sediments. *Sci. Total Environ.* **607**–**608**, 23–31, <https://doi.org/10.1016/j.scitotenv.2017.06.187> (2017).
- Oswald, K. *et al.* Methanotrophy under versatile conditions in the water column of the ferruginous meromictic Lake La Cruz (Spain). *Front. Microbiol.* **7**, 1762, <https://doi.org/10.3389/fmicb.2016.01762> (2016).
- del Giorgio, P. A. & Peters, R. H. Balance between Phytoplankton Production and Plankton Respiration in Lakes. *Can. J. Fish. Aquat. Sci.* **50**(2), 282–289, <https://doi.org/10.1139/f93-032> (1993).
- Xing, F. & Heinz, S. Temperature and Dissolved Oxygen Simulations for a Lake with Ice Cover. St. Anthony Falls Hydraulic Laboratory; Retrieved from the University of Minnesota Digital Conservancy: Minnesota, 1994.
- Martinez-Cruz, K. *et al.* Ubiquitous and significant anaerobic oxidation of methane in freshwater lake sediments. *Water Res.* **144**(2), 332–340, <https://doi.org/10.1016/j.watres.2018.07.053> (2018).
- Deutzmann, J. S., Stief, P., Brandes, J. & Schink, B. Anaerobic methane oxidation coupled to denitrification is the dominant methane sink in a deep lake. *P. Natl. A. Sci.* **111**(51), 18273–18278, <https://doi.org/10.1073/pnas.1411617111> (2014).
- Valenzuela, E. I. *et al.* Electron shuttling mediated by humic substances fuels anaerobic methane oxidation and carbon burial in wetland sediments. *Sci. Total Environ.* **650**, 2674–2684, <https://doi.org/10.1016/j.scitotenv.2018.09.388> (2019).
- Bižić, M. *et al.* Aquatic and terrestrial cyanobacteria produce methane. *Sci. Adv.* **6**(3), eaax5343, <https://doi.org/10.1126/sciadv.aax5343> (2020).
- Hofmann, H. Spatiotemporal distribution patterns of dissolved methane in lakes: How accurate are the current estimations of the diffusive flux path? *Geophys. Res. Lett.* **40**(11), 2779–2784, <https://doi.org/10.1002/grl.50453> (2013).
- Streletskiy, D., Anisimov, O. & Vasiliev, A. Permafrost Degradation. In *Snow and Ice-Related Hazards, Risks and Disasters*; Elsevier, **10**, 303–344; <https://doi.org/10.1016/B978-0-12-394849-6.00010-X> (2015).
- Kankaala, P., Huotari, J., Peltomaa, E., Saloranta, T. & Ojala, A. Methanotrophic activity in relation to methane efflux and total heterotrophic bacterial production in a stratified, humic, boreal lake. *Limnol. Oceanogr.* **51**(2), 1195–1204, <https://doi.org/10.4319/lo.2006.51.2.1195> (2006).
- French, R. H., Cooper, J. J. & Vigg, S. Secchi Disc Relationships. *J. Am. Water Resour. Assoc.* **18**(1), 121–123, <https://doi.org/10.1111/j.1752-1688.1982.tb04538.x> (1982).
- LaPerriere, J. D. & Edmundson, J. A. Limnology of two lake systems of Katmai National Park and Preserve, Alaska: Part II. Light penetration and Secchi depth. *Hydrobiologia* **418**(1), 209–216 (2000).
- Hornibrook, E. R., Longstaffe, F. J. & Fyfe, W. S. Evolution of stable carbon isotope compositions for methane and carbon dioxide in freshwater wetlands and other anaerobic environments. *Geochim. Cosmochim. Ac.* **64**(6), 1013–1027, [https://doi.org/10.1016/S0016-7037\(99\)00321-X](https://doi.org/10.1016/S0016-7037(99)00321-X) (2000).

## Acknowledgements

The authors are thankful to Victoria T. Velázquez-Martínez, Juan Corona-Hernández, and David Flores-Rojas for their technical assistance, Anatoli Pimov for his logistical help in the field, I. Moussa and D. Dalger for  $\delta^{13}\text{C}$ -DIC analysis which was performed at the SHIVA analytical platform, as well as F. Julien, D. Lambrigt and V. Payre-Suc for DOC and major elements analysis performed at the PAPC platform (EcoLab laboratory). The authors declare that they have no conflicts of interest. This work was supported by ERANET-LAC project METHANOBASE

(ELAC2014 DCC-0092), (ECOS Sud-Conicyt Project “MATCH” C16B03, Consejo Nacional de Ciencia y Tecnología Project 255704). We also gratefully acknowledge Conacyt for the financial support to Oscar Gerardo-Nieto (grant # 277238). A.S.-J. used funding time for writing from FONDAP/CONICYT 15110009 and NEXER-UMAG-Carbon Dynamics in the Anthropocene: A perspective from Extreme Environments.

### Author contributions

F.T. conceived the study. F.T. and A.S.-J. wrote the manuscript. N.T., R.T., and M.S.A.-E. organized the field campaign and logistics. F.T., K.M.-C. A.S.-J., L.G. and O.G.N. conducted field sampling and chemical lab analysis. M.B. and L.C. contributed equal to this work. L.C., M.B., and C.L., conducted molecular biology analysis. The manuscript was revised and edited through contributions of all authors. All authors have given approval to the final version of the manuscript.

### Competing interests

The authors declare no competing interests.

### Additional information

**Supplementary information** is available for this paper at <https://doi.org/10.1038/s41598-020-60394-8>.

**Correspondence** and requests for materials should be addressed to A.S.-J.

**Reprints and permissions information** is available at [www.nature.com/reprints](http://www.nature.com/reprints).

**Publisher’s note** Springer Nature remains neutral with regard to jurisdictional claims in published maps and institutional affiliations.



**Open Access** This article is licensed under a Creative Commons Attribution 4.0 International License, which permits use, sharing, adaptation, distribution and reproduction in any medium or format, as long as you give appropriate credit to the original author(s) and the source, provide a link to the Creative Commons license, and indicate if changes were made. The images or other third party material in this article are included in the article’s Creative Commons license, unless indicated otherwise in a credit line to the material. If material is not included in the article’s Creative Commons license and your intended use is not permitted by statutory regulation or exceeds the permitted use, you will need to obtain permission directly from the copyright holder. To view a copy of this license, visit <http://creativecommons.org/licenses/by/4.0/>.

© The Author(s) 2020